Shivakumar Gouda, P. S., Williams, J. D., Yasaee, M., Chaterjee, V., Jawali, D., Rahatekar, S., & Wisnom, M. R. (2016). Drawdown prepreg coating method using epoxy terminated butadiene nitrile rubber to improve fracture toughness of glass epoxy composites. *Journal of Composite Materials*, *50*(7), 873-884. https://doi.org/10.1177/0021998315583317

Draw-down Pre-preg coating method using Epoxy Terminated Butadiene Nitrile Rubber to Improve Fracture Toughness of Glass Epoxy Composites

P S Shivakumar Gouda[1,2,4*], John D Williams[1],Mehdi Yasaee[1], Vijay Chatterjee[3] Dayananda Jawali[4] Sameer S Rahatekar[1,5*] M.R Wisnom[1]

[1]Advanced Composites Centre for Innovation & Science (ACCIS), University of Bristol, BS8 1TR,UK

[2]SDM College of Engineering & Technology, **VTU,**Dharwad, 580 002, India

[3]School of Chemistry, University of Bristol, BS8 1TS, United Kingdom

[4]Dept. of Mechanical Engineering, S.J. College of Engineering, Mysore - 570 006, India

[5]Centre for Nano Science and Quantum Information, University of Bristol, BS8 1FD, UK

ABSTRACT

*Laminates of fibre reinforced pre-preg have excellent in-plane mechanical properties, but have inadequate performance in the through thickness direction. Here, we address this issue by application of epoxy terminated butadiene nitrile (ETBN) liquid rubber between the pre-preg laminae using an automatic draw bar coating technique. Test results reveal that by adding ETBN in small quantities in the range of 9.33 g/m^2 to 61.33 g/m^2, the interlaminar critical energy release rates (G_{Ic} and G_{IIc}) are improved by up to 122% in mode-I and 49% in mode-II. Moreover, this finding is further supported by the DMA thermograms clearly indicates that coating is not altered the T_g of ETBN coated samples.SEM analysis of fracture surfaces showed that rubber particles formed micro cavitations in the epoxy, causing localised **rubber rich** regions. These resin rich regions require more energy to fracture, resulting in increased toughness of the glass epoxy pre-preg systems.*

Keywords:*Polymer–matrix composites (PMCs), Particle-reinforcement, Fracture toughness,* ***Pre-preg coating.***

***Correspondence Authors:**

1.P.S.Shivakumar Gouda: ursshivu@gmail.com

2. Sameer S Rahatekar; Sameer.Rahatekar@bristol.ac.uk

1. Introduction

Polymer composites are extensively used not only in the aerospace industry, but also in marine, automotive, and civil engineering applications. For laminated composites, delamination tends to be the dominant failure mode in service, which results in the unacceptable reduction of material performance. Therefore, modifying the interlaminar fracture toughness of high-performance composites, especially for composites with brittle matrices, is an essential task for the use of these materials in safety critical applications. Studies exist in the literature addressing the improvement of interlaminar fracture toughness, through fibre-stitching, interleaving tough constituents, [1,2] through thickness z–pinning, and parent matrix resin coating, between the plies [3]. These methods work on the macro scale and each of these has its own merits and disadvantages compared to the methods developed in our previous work for CNT and rubber coating on pre-pregs which has been[4, 5] extended in this paper for dispersing ETBN rubber on to the glass epoxy pre-preg system. For instance, dispersing rubber particles directly into the epoxy matrix [6-11] significantly improve fracture toughness whilst retaining the bulk properties of the epoxy system. To enhance the fracture toughness of composites, Yan *et al.* [12] studied the toughening mechanisms of reactive liquid rubber carboxyl terminated butadiene nitrile (CTBN) and core shell rubber (CSR) dispersed in the bulk epoxy of the composite laminate. It was observed that particle cavitation did not occur and that the main toughening mechanism was large plastic deformation near the crack-tip due to the contribution of rubber domains in the matrix, which lowered the yield strength and increased elongation. However previous observations [12-13] have shown that the cavitation resistance of the rubbery phase does not play any role in the toughening mechanism of the epoxy matrix studied [14] and that the improvement was due to an increase of the thickness of the inter-layer between plies. As the inter-layer thickness increases beyond the plastic zone area, the crack will no longer propagate along the ply interface of the host matrix and the fibres will remain within the resin resulting in

cohesive failure of the inter-layer [7]. The saturation of the plastic yield zone has been shown to occur for insert thicknesses of>0.1mm for thermoset resins [15].Improvement in fracture toughness using reactive liquid rubber particles CTBN was reported in [15, 16], but only under mode-I loading. These methods are more expensive and time consuming to disperse rubber in fibre epoxy composites as compared to the new method of dispersing rubber in pre-pregs shown here.Fibre-bridging is a quite important phenomenon for the interlaminar fracture toughness, particularly in delamination opening mode. The fibre bridging occurs when fibres are pulled from one side of the delamination plane to the other side. The interlaminar fracture toughness will be increased by the occurrence of fibre-bridging [17-19].

The present work utilises a solvent based method of dispersing ETBN liquid rubber to coat aerospace grade pre-pregs using an automated draw down process. This is a simple, and rapid alternative method as discussed earlier to incorporate rubber in carbon fibre reinforced epoxy pre-preg system as discussed in our previous work [5], but our study was limited to mode-I and mode-II fracture toughness. This method is more efficient than the use of costly and time consuming dispersion techniques [20 - 25] making it potentially scalable for large scale manufacturing. This investigation aims to study the experimental assessment of fracture behaviour and ETBN dispersion and its pre-preg coating process through SEM, DMA and FT-IR spectra.

2. Experimental

2.1 Materials and Rubber solutions

Standard aerospace grade unidirectional E-Glass-913 epoxy pre-preg(Hexcel UK) was used in this study. The coating material was epoxy-terminated butadiene-nitrile rubber Hypro^{TM} 1300X63(Emerald Performance Materials, UK), containing 26% acrylonitrile. To produce the solutions for draw down coating ETBN rubber was manually mixed with 60ml of

tetrahydrofuran (THF) until a clear solution was made. Details of the rubber content used in the tests are shown in Table.1.

2.2. Preparation of ETBN rubber modified glass epoxy laminates

The ETBN rubber /THF solution was applied to one end of the surface of the E-glass pre-preg (170mm x 150mm) using a pipette. By using an automated draw down coating machine as illustrated in Fig.1 (draw bar wire gauges: 0.2mm, 0.5mm for DCB samples and 0.2mm, 0.5mm, 0.8mm for ENF samples)the solution was drawn across the pre-preg to produce a fine coating of ETBN rubber / THF solution in very little time as compared to dispersing rubber into epoxy by lowering the viscosity and then infusing in to mould to make the composites [5].

A chemical handling fume-hood was used to take away the THF fumes present on the pre-preg ply safely. After evaporation of the solvent, a thin layer ETBN formed on pre-preg ply surface (Figure 1(b)).This ply with the ETBN coating on one surface on top was laid-up with 12unmodified plies above and 11 below (all oriented at 0^{o}) such that a 24-ply laminated is formed with the rubber coating at the central inter-layer. The laminate was then bagged and cured (125^{o}C for 1 hour at 7 bar) in an autoclave in accordance with the manufacturer's curing specifications. Finally, DCB and ENF samples were cut in accordance with ASTM D5528-01 and JIS K 7086 standards respectively. **Table 2** shows the four different ETBN rubber solution concentrations used and the resulting coating densities measured for the different draw bars used.

Figs.2(a) and (b), show optical micrographs of ETBN rubber on the pre-preg before and after coating. The pre-preg in Fig. 2(b) shows the quality of the coating before curing as the epoxy resin and glass fibres are uniformly covered with a fine coating of ETBN rubber, with a thickness of approximately 0.1mm.

Fig.3 shows the cross section of the cured specimen of epoxy/glass fibre composites and ETBN modified glass/epoxy composites. The circular objects seen in the figure 3a-d are the cross-section of glass fibres. In the glass fibre epoxy composite (without addition of ETBN) cross-section (Fig 3(a)), individual ply boundaries can be identified surrounded by resin rich layers (as shown by enhanced pink colour region). After the ETBN rubber coating on glass/epoxy pre-pregs, the ETBN infiltrate through the thickness of glass fibre pre-preg during autoclave curing (the ETBN filtration zone is shown by enhanced pink region in Fig 3b-d).This infiltration depth varies between 50μm and 100μm in all specimens and appears not to be affected by the density of rubber coating. As a result of this infiltration, the average global thickness of the coated composite samples increased by a very small amount in the range $\sim$ 20- 30μm, although this thickness variation that might be expected between autoclave cured laminates [26].

3 Test procedures

3.1 Dynamic mechanical analysis (DMA)

The viscoelastic properties of the coated and uncoated epoxy glass pre-preg laminates were measured using a dynamic mechanical thermal analyzer (DMA) developed by TA instruments Japan. **The samples were cured at 125^{o}C for 1 hour at 7 bar in autoclave** and the analysis was done in a dual cantilever measuring system and is similar to 3-point bending except that the ends of the sample are clamped. The samples were heated from 0 to 250^{0}C at the heating rate of 3^{0}C/min. The frequency used was 1 Hz.

3.2 Fracture test

Mode I double cantilever beam (DCB) experiments were conducted in accordance with ASTM-D5528 [26]. Using a calibrated 1kN Instron 3343 uni-axial testing machine, displacement was applied to the sample at a crosshead extension rate of 3mm/min. Five DCB

specimens for each coating configuration were tested. The geometry of the DCB is shown in Fig. 4.

For the DCB tests, crack growth was recorded using a digital video camera to a resolution of $\pm$ 0.5 mm. The mode-I critical strain energy release rate (G_{Ic}) was determined using modified beam theory as per the ASTM-D5528 standard. The load (P) and extension (δ) were recorded for every 1mm increment in crack length up to 5mm with continued crack growth monitored and recorded in 5mm increments until the crack length reached a total length of 110mm.

The mode-I initiation and propagation fracture toughness were calculated using the visual method by Eq. (1) [27]

$$G_{Ic} = \frac{3P\delta}{2B(a+|\Delta|)} \qquad (1)$$

Where P: the load, d: the load point displacement, B: the specimen width, a: the delamination length, h: the specimen thickness and Δ: correction factor to account for rotation of the DCB arms. Δ: was determined experimentally in accordance with ASTM D5528-01 by drawing a least squares plot of the cube root of compliance ($C^{1/3}$) as a function of delamination length.

Mode-II end notch flexural (ENF) experiments were conducted in accordance with the Japanese Industrial Standard (JIS K 7086) for unidirectional (UD) composites. ENF samples were loaded as per the diagram shown in **Fig.5 (a)** with a constant displacement rate of 3mm/min. To prevent the possibility of a high critical strain energy release rate (G_{IIc}) due to a resin rich pocket ahead of the pre-crack insert, a natural mode-II pre crack was generated by initial loading of the sample until crack growth was observed, then by unloading and moving the sample to a new position as shown in **Fig.5 (b),** at which point the testing was begun. For both cases, the specimen was positioned such that the initial crack length $a_0$was 25mm from the left roller support.

The mode-II fracture toughness was then calculated using Eqn.(2) &(3) [28]:

$$G_{IIC} = \frac{9\, a_1^2 P_C^2 C_1}{2B(2L^3+3a_1^3)} \quad (2)$$

$$\text{where } a_1 = \left[\frac{C_1}{C_0}a_0^3 + \frac{2}{3}\left(\frac{C_1}{C_0} - 1\right)L^3\right]^{1/3} \quad (3)$$

Where a_1 is the modified crack length calculated using Eq.(3) P_C, is the initial critical load, C_1 and C_0 are the load-point compliances at the initial elastic and initial critical loads respectively. B is the width of the specimen (mm) and L is the distance between supporting point and loading point (mm). For both test procedures, five specimens of each coating configuration were tested.

3.3 Scanning electron microscopic (SEM) analysis

Fracture surfaces of DCB and ENF specimens were carefully cut using a diamond blade cutting wheel and all samples were silver sputter coated prior to SEM analysis to prevent build up surface charge. A JEOL 5600 LV SEM was used to study the surface morphology of the samples.

4. Results and Discussion

4.1DMA studies

The storage modulus (E) and the loss factor, tan δ, of the epoxy glass control and the composites with different ETBN aerial coating densities are shown in **Figs. 6 and 7 respectively.** At low temperatures, all the samples show a very high elastic modulus, followed by slight drops due to second-order transitions between 50 and 100^{o}C**(Fig. 6).** The major drop in the temperature range of 175 – 200^{o}C due to the glass transition, is evident for all samples.

In this temperature range, the tan δ curves show a peak indicating the glass transition temperature (T_g) of the material. The ETBN coated samples with coating densities of 9.33 g/m^2 and 34.66 g/m^2 also show similar T_g as that of the glass control (**Fig. 7**).The change in

storage modulus and T_g of ETBN coated and un-coated pre-preg laminate samples is reported in Table 3. As far as the storage modulus is concerned, a slightly higher value in the glass control sample can be observed, as reported in Table 3.Further, a decrease in elastic modulus as observed from temperature 100^{o}C to 250^{o}C for all the samples.

4.2Fracture Toughness

The representative load vs. deflection curves for the DCB specimens with and without ETBN rubber coatings are plotted in **Fig.8(a).**The rubber coated samples show a large increase (≈ 55%) in load before the crack starts to propagate compared to the control sample. In **Fig.8 (b),** representative delamination resistance curves are shown for each sample. There is a large increase in the fracture toughness of the rubber coated specimens as the crack progresses, although a limit appears to be reached at 29.77 g/m^2 as delamination resistance reduces slightly at 34.66 g/m^2. Similar enhancement in the fracture toughness is reported in [5] for ETBN modified UD carbon epoxy pre-preg laminates.

A summary of the results is shown in **Fig.9**.G_{IC}values shown in **Fig.9 (a)** are considerably higher with a value of 610 J/m^2 for the ETBN rubber coated samples with aerial density of 29.77 g/m^{2}with respect to baseline G_{IC} of 274 J/m^2. Similarly, the propagation strain energy release rate G_{IP} was found to be 933 J/m^2 for the rubber coating density of 29.77 g/m^2. However the G_{IP} value reduced by 5% with increase in ETBN coating density to 34.66 g/m^{2}as shown in **Fig.9 (b).**The lower coating density to 9.33 g/m^{2}gave lower G_{IC} and G_{IP} values compared to samples coated with higher coating density, but still higher than the controls.

It was observed from the resistance curves that crack propagation was stable and constant, with no crack jumps between crack lengths of 60 and 110mm for all the ETBN modified samples. It can also be seen that approximately 10mm of mode I delamination propagation is

necessary to realise the full toughening effect of the ETBN particles in a GFRP composite, compared to control samples.

The flexural modulus (E_{1f}) of each specimen was calculated according to the ASTM D5528-01 standard. Mean values are displayed in **Fig.10**. Mean E_{1f} values of each coating density show similar flexural modulus for all of the rubber modified samples, relative to control samples, within the accuracy of measurements.

Table 4 compares results from other studies using rubber toughening agents and their effectiveness. It can be seen that this draw down approach has performed slightly better than the direct mixing approach for similarly loaded specimens.

Fig.11 (a) shows typical load displacement plots and corresponding averaged results for mode-II (note for the 9.33 g/m^2 and 34.66 g/m^{2}ETBN coated cases, samples where positioned with an initial crack length of 35mm instead of 25mm, due to this a small change in peak loads can be observed in load displacements curves in **Fig. 11(a),** but this has no effect on the fracture toughness results).

It can be seen in **Fig.11(b)** that the baseline control specimens have an average $G_{IIC}$of 943J/m^2, in close agreement to the results of Schuecker and Davidson [31]. The application of the ETBN coating clearly increased the G_{IIC} of the pre-preg system in all cases, by up to 49%. The observation of the modified samples showed stable crack propagation for a short length before an unstable crack jump. There appears to be a slight decrease in the mode II toughness with increase in rubber coating density.

4.3 SEM analysis

To enhance our understanding of the ETBN rubber toughening mechanisms responsible for the increase of the mode-I and mode-II fracture toughness of UD glass epoxy pre-preg laminate system, fracture surfaces of each sample were examined.

Unmodified DCB fracture surfaces (Fig.12a) show a common cusp formation of the resin between the fibres. Fracture surfaces of samples with an ETBN rubber coating of 9.33g/m^2(Fig.12b) show the formation of rubber particles within the rubber phase. The improved fracture toughness of the rubber modified samples with respect to the unmodified samples is due to tri-axial stress on the rubbery particles leading to cavitations within the particles and plastic void growth around the cavitated particles as observed in Fig 12 b, and improved fibre bridging in the ETBN coated samples (Fig. SI-2).

A further increase of rubber density to 29.77g/m^2 **(Fig.12c)** resulted in a minor increase in fracture toughness as slightly more micro rubber cavities were observed. A small additional increase of the rubber density to 34.66g/m^2 resulted in a considerable amount of uneven and rough resin fracture surfaces with almost no visible fibres **(Fig.12d).** This in fact gives a slightly reduced initiation G_{IC} of the material with little change in the G_{IP} relative to the 29.77g/m^2 rubber density. This suggests that a maximum toughness improvement has been reached with rubber density of approximately 30g/m^2.

Similarly, the fracture surfaces of the mode-II samples shown in **Fig.13** indicate the toughening mechanism of ETBN rubber in epoxy pre-preg systems. SEM micrographs for unmodified samples **(Fig.13a)** show shear cusps between fibres, commonly observed with mode II fracture surfaces of brittle composites [2]. In comparison, with the ETBN rubber modified pre-preg laminated samples, there appears to be far more resin residue around the fibre surfaces surrounding micro cavities. This shows that the presence of rubber particles in glass epoxy pre-pregs has allowed for localised micro **rubber rich** regions to be formed.

Specimens with a lower rubber coating density of 34.66 g/m^2**(Fig.13b)** appear to show fewer rubber cavities than specimens with higher rubber concentration (Fig 13(c) and (d)).The increase in rubber content in mode-II samples showed (Fig.11a and 11b) no further improvement in mode-II fracture energy release rate.

5. Conclusions

In this study we examined the mode I and mode II fracture toughness of a UD glass epoxy pre-preg system with and without ETBN rubber ply surface modification. A simple and rapid method of rubber dispersion on the pre-preg surface was, achieved with the aid of the automated draw down coating technique. Storage modulus, elastic modulus and T_g were similar in ETBN coated and un-coated glass pre-preg composites. This technique thus aided accurate measurement of the effect of pre-cure coating thickness as well as rubber content on the mode I and mode II fracture toughness of the glass epoxy composite system. Storage modulus, elastic modulus and T_g are similar in ETBN coated and un-coated glass pre-preg composites. FT-IR spectra data reveals good interaction between epoxy glass pre-preg and ETBN on the basis of the change in IR absorption peak shape and position.

The modified pre-preg system saw improvement of both the mode-I initiation fracture toughness (G_{IC}) and the steady state propagation fracture toughness (G_{IP}) of up to 122% using ETBN rubber in the case of a coating density of 29.77 g/m^2. The flexural modulus of the rubber modified UD glass epoxy pre-preg systems was shown to be similar to the un-modified pre-preg.

The mode-II interlaminar fracture toughness (G_{IIC}) saw an improvement of 49% for an ETBN coating density of 9.33 g/m^2. However increases in the ETBN coating density to 44 and 61.33 g/m^2, resulted in similar or slightly reduced mode II toughness.

SEM fractography of ETBN modified UD glass epoxy pre-preg systems showed micro rubber particle cavities in the matrix. Surrounding these cavities was evidence of rough lumps of fractured resin residue for both mode I and mode II fracture surfaces. This shows that the presence of elongated rubber cavities on the fracture surfaces and the amount of fibre bridging (Fig.SI-2) in ETBN coated samples require more energy to fracture and thus contributed to increasing the interlaminar fracture toughness. However, in mode II tests, the increased ETBN content was insignificant on G_{IIC} values.

To achieve optimum improvements in fracture toughness in both mode-I and mode-II using ETBN pre-preg,a coating density of 29.77 g/m^2 is recommended as a good compromise.

Acknowledgements

The authors would like to thank the Commonwealth Scholarship Commission UK and ACCIS, and the Centre for Nano Science and Quantum Information (NSQI), University of Bristol, UK for providing the scholarship and facilities. Authors also would like to acknowledge support from UK India Educational Research Initiative (UKIERI) program.

References

[1] Yasaee M, Bond IP, Trask RS, Greenhalgh ES. Mode I interfacial toughening through discontinuous interleaves for damage suppression and control. Composites Part A: Applied Science and Manufacturing 2012; 43:198–207.

[2] Yasaee M, Bond IP, Trask RS, Greenhalgh ES. Mode II interfacial toughening through discontinuous interleaves for damage suppression and control. Composites Part A: Applied Science and Manufacturing 2012; 43: 121–128.

[3] Shafiullah Khan and Jang-Kyo Kim. Impact and Delamination Failure of Multi-scale Carbon Nanotube-Fiber Reinforced Polymer Composites. A Review. Int'l J. of Aeronautical & Space Science 2011; 12: 115–133.

[4] John Williams,NeilGraddage, Sameer Rahatekar. Effects of plasma modified carbon nanotube interlaminar coating oncrack propagation in glass epoxy composites. Composites part A 2013; 54: 173-181.

[5] Shivakumar Gouda. P. S, Vijay Chatterjee, Barhai P. K, DayanandaJawali, Sameer Rahatekar, Wisnom M. R. Improved fracture toughness in Carbon fibre epoxy composite through novel pre preg coating method using Epoxy Terminated Butadiene Nitrile rubber. Materials and Design 2014; 62: 320-326.

[6] Kinloch A. J. Toughening Epoxy Adhesives to Meet Today's Challenges. MRS Bulletin 2003; 28: 445-448.

[7] Hojo M, Ando T, Tanaka M, Adachi T, Ochiai S, Endo Y. Modes I and II interlaminar fracture toughness and fatigue delamination of CF/epoxy laminates with self-same epoxy interleaf. International Journal of Fatigue 2006; 28:1154-1165.

[8] Verchere D, Sautereau H, Pascault J. P.,Moschiar S. M., RiccardiCand Williams R. J. J. Miscibility of Epoxy Monomers with Carboxyl-Terminated Butadiene Acrylonitrile Random Copolymers. Polymer 1989; 30: 107-115.

[9] Pearson R. A and Yee A. F. Toughening Mechanisms in Elastomer-Modified Epoxies: Part 2 - Microscopy Studies. Journal of Materials Science 1986; 21: 2475-2488.

[10] Kinloch A. J, Shaw, S. J., Tod D. A,Hunston D. L. Deformation and Fracture Behaviour of a Rubber-Toughened Epoxy.Part-1-Microstructure and Fracture Studies. Polymer 1983; 24: 1341-1354.

[11] Kinloch A. J., Shaw S. J.,Hunston D. L. Deformation and Fracture Behaviour of a Rubber-Toughened Epoxy.II. Failure Criteria. Polymer 1983; 24: 1355-1363.

[12] Yan C., Xiao, K., Ye L. and Mai Y.W. Numerical and Experimental Studies on the Fracture Behaviour of Rubber-toughened Epoxy in Bulk Specimen and Laminated Composites. Journal of Materials Science 2002;37: 921-927.

[13] Bagheri Reza, Raymond A. Pearson. Role of particle cavitation in rubber-toughened epoxies 1. Micro void toughening. Polymer 1996; 37: 4529-4538.

[14] Singh S, Partridge IK. Mixed-mode fracture in an interleaved carbon-fibre/epoxy composite. Composites Science and Technology 1995; 55: 319-327.

[15] Sela N, Ishai O, Bankssills L. The effect of adhesive thickness on interlaminarfracture toughness of interleaved CFRP specimens. Composites 1989; 20: 257-264.

[16] M.R. Dadfar, F. Ghadami.Effect of rubber modification on fracture toughness properties of glass reinforced hot cured epoxy composites. Materials and Design 2013; 47: 16–20.

[17] Huang X.N, Hull D. Effects of fibre bridging on G_{IC} of a unidirectional glass/epoxy composite. Composites Science and Technology 1989; 35: 283-299.

[18] Madhukar M.S, Drzal L.T. Fibre-matrix adhesion and its effect on composite mechanical properties: IV. Mode I and Mode II fracture toughness of graphite/epoxy composites, Journal of Composite Materials 1992; 26: 936-968

[19] Petrie E. M. Important Considerations Regarding Adhesion to Plastics – Part I-Thermosetting Plastics, 2007

[20] Tsai J. N, Huang B. H, Cheng Y. L. Enhancing Fracture Toughness of Glass/Epoxy Composites by Using Rubber Particles Together with Silica Nanoparticles. Journal of Composite Materials 2009; 43:1-17.

[21] Salinas-Ruiz, Maria D. M., Alex A. Skordos,Ivana K. Partridge. Rubber- toughened epoxy loaded with carbon nanotubes: structure-property relationships. Journal of materials science 2010; 45: 2633-2639.

[22] Eric N. Gilbert, Brian S. Hayes, James C. Seferis, Interlayer toughened unidirectional carbon pre-preg systems: effect of preformed particle morphology. Composites: Part A 2003; 34: 245–252.

[23] Brian S. Hayes, James C. Seferis, Toughened Carbon Fiber Pre-pregs Using Combined Liquid and Preformed Rubber Materials. Polymer Engineering and Science 2001; 41:170.

[24] MatthieuNobelen, Brian S. Hayes, James C. Seferis, Influence of Elastomer Distribution on the Cryogenic Microcracking of Carbon Fiber/Epoxy Composites. Journal of Applied Polymer Science 2003; 90: 2268–2275.

[25] Brian S. Hayes, James C. Seferis, Influence of Particle Size Distribution of Preformed Rubber on the Structure and Properties of Composite Systems. Journal of Composite Materials 2002; 36: 299-312

[26] Matthew M. Thomas, Babu Joseph, and John L. Kardos. Experimental Characterization of Autoclave-Cured Glass-Epoxy Composite Laminates: Cure Cycle Effects Upon Thickness, Void Content, and Related Phenomena. Polymer Composites 1997; 18: 283-299.

[27] ASTM-D5528-01. Standard test method for mode-I interlaminar fracture toughness of unidirectional fiber-reinforced polymer matrix composites. ASTM International, 2007.

[28] JIS K 7086 Japanese Industrial Standard testing methods mode-I, mode II interlaminar fracture toughness of carbon fiber reinforced plastics 1993.

[29] ChikhiN,Fellahi S, BakarM. Modification of epoxy resin using reactive liquid (ATBN) rubber. European Polymer Journal 2002; 38: 251-264.

[30] MawhinneyD.B. Infrared spectral evidence for the etching of carbonnanotubes: ozone oxidation at 298 K. Phys. A, 1998. 67: 29.

[31] Schuecker C, Davidson BD. Evaluation of the accuracy of the four-point bend end-notched flexure test for mode II delamination toughness determination. Composite Science and Technology 2000; 60: 2137-2146.

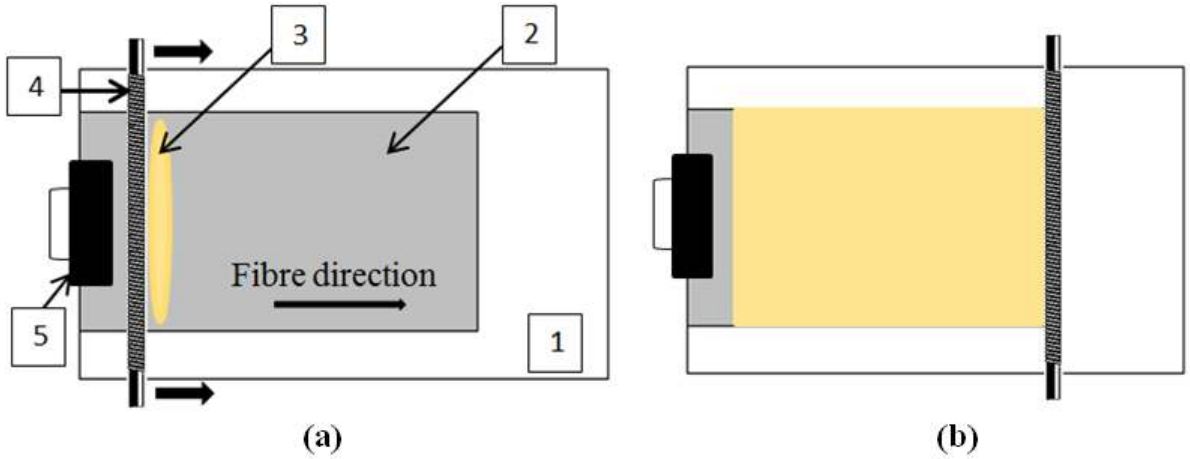

1. Glass plate 2. Pre-preg ply 3. ETBN rubber solution 4. Draw bar 5. Clip

Fig 1. Schematic of drawn down coating equipment

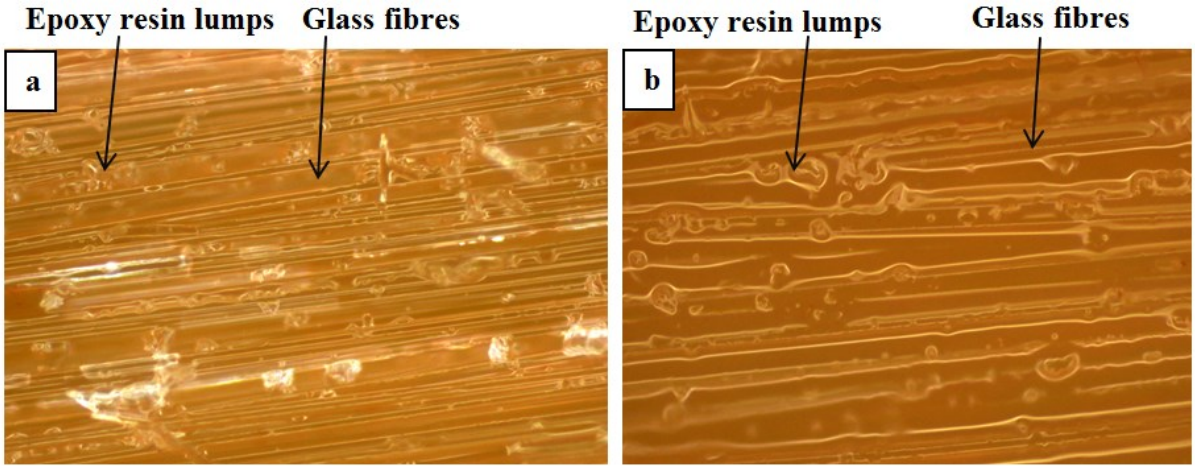

Fig 2 Pre-preg surface (a) Before coating (b) After coating

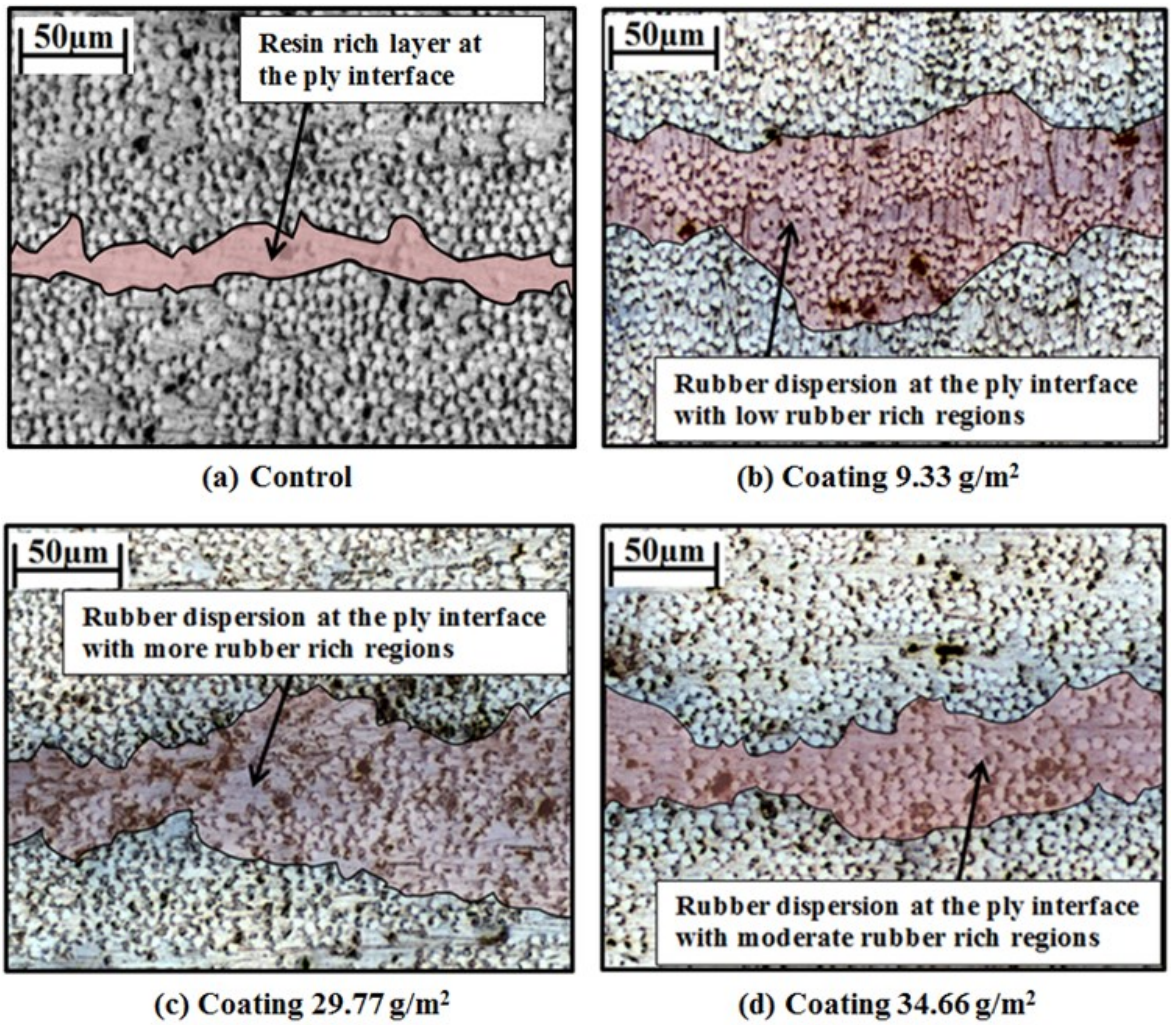

Fig. 3 Optical micrographsshowing cross section of the specimens, viewing normal to the fibers, showing resin rich layers, appearing in most of the glass control specimens at the ply interface. Rubber dispersion at ply interface as and rubber infiltration into plies highlighted.

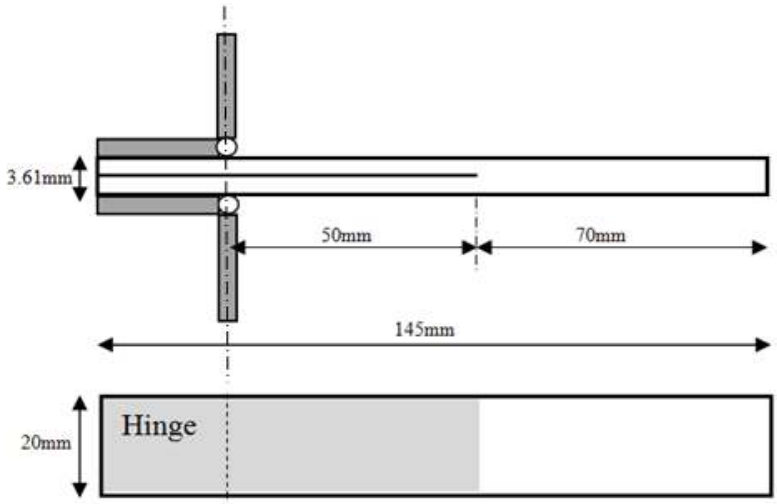

Fig 4 DCB Specimen geometry

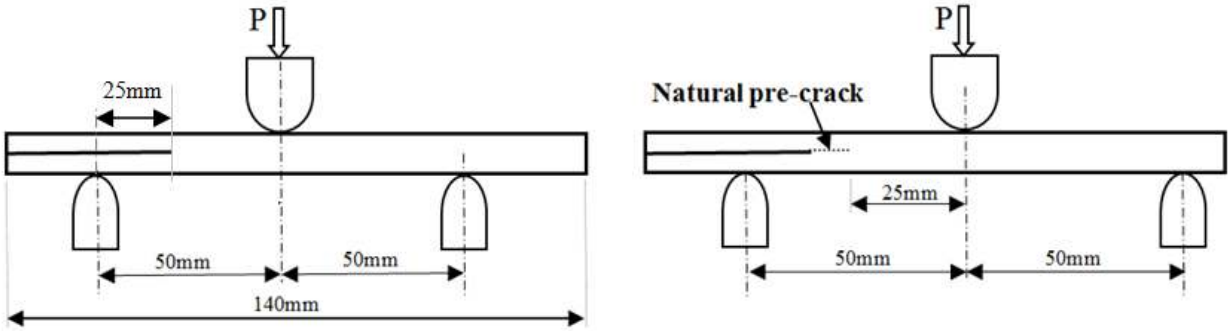

Fig. 5(a) **Fig.5(b)**

Fig.5 Three point ENF specimen loading configuration showing (a) initial loading setup (b) final loading set up with natural mode-II pre crack.

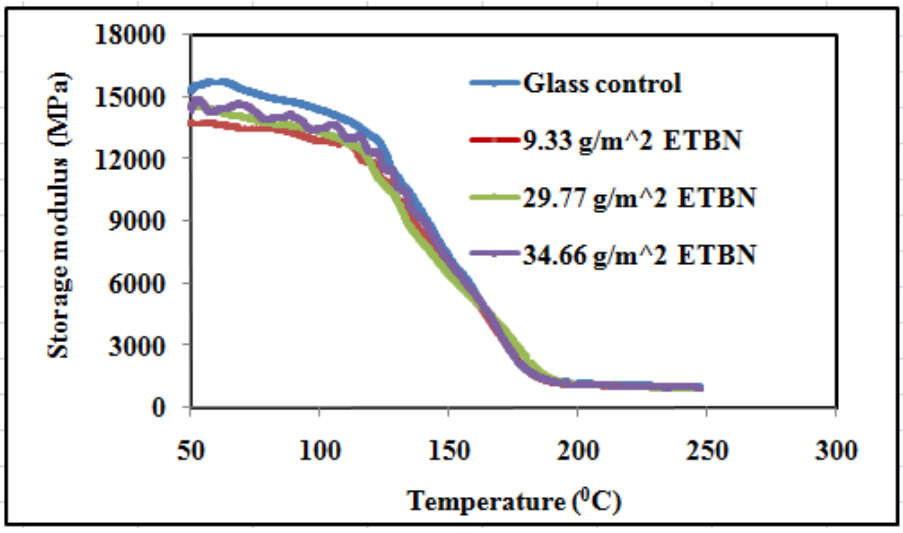

Fig. 6 Storage modulus versus temperature of the epoxy glass 913 pre-preg laminates and its ETBN coated laminates with different aerial coating densities

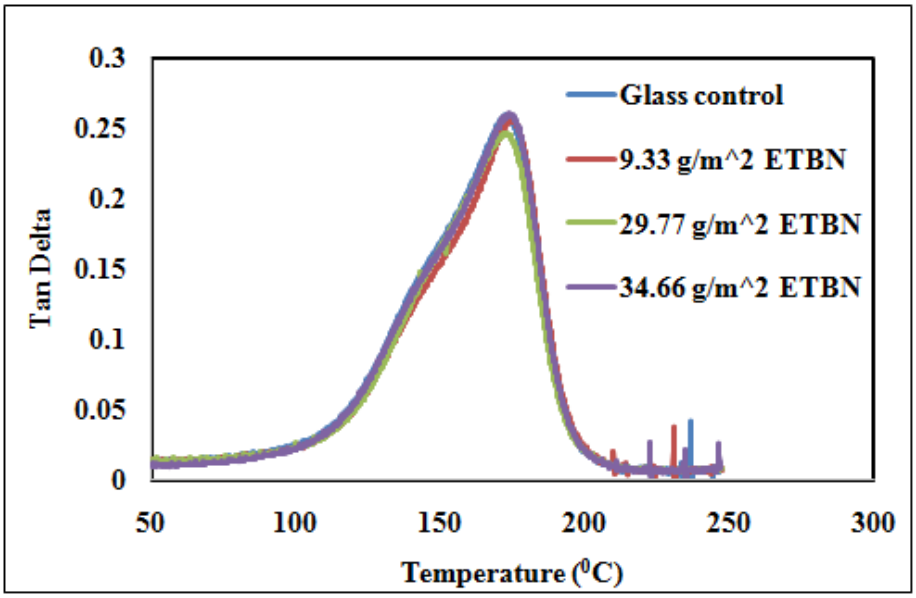

Fig. 7 Loss factor (tan δ) versus temperature for the glass control samples and its ETBN modified composites with different aerial coating densities.

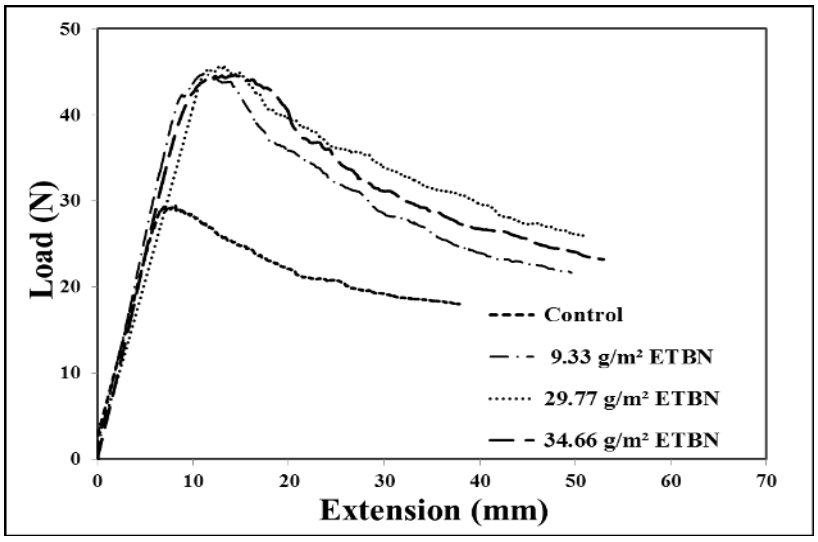

(a)

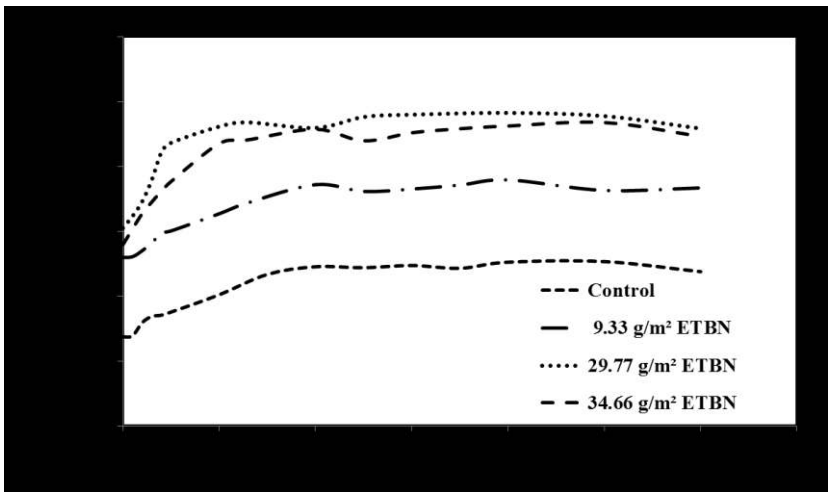

(b)

Fig 8.(a)Load vs. displacement curves for both control and rubber modified DCB (b) Mode-I interlaminar fracture toughness (G_I)values vs. crack length

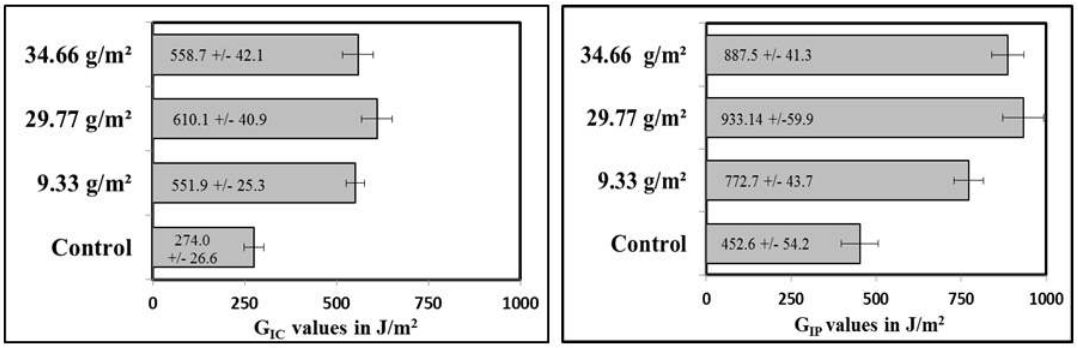

(a) **(b)**

Fig 9. Mode-I Interlaminarfracture toughness (a) G_{IC} values (b) G_{IP} values (error bars with standard deviation, minimum of 5 samples per data point).

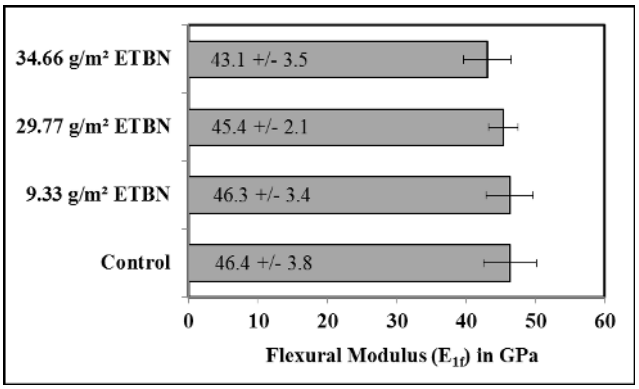

Fig 10. Flexural modulus (E_{1f}) of control and ETBN coated DCB samples (error bars with standard deviation, minimum of 5 samples per data point).

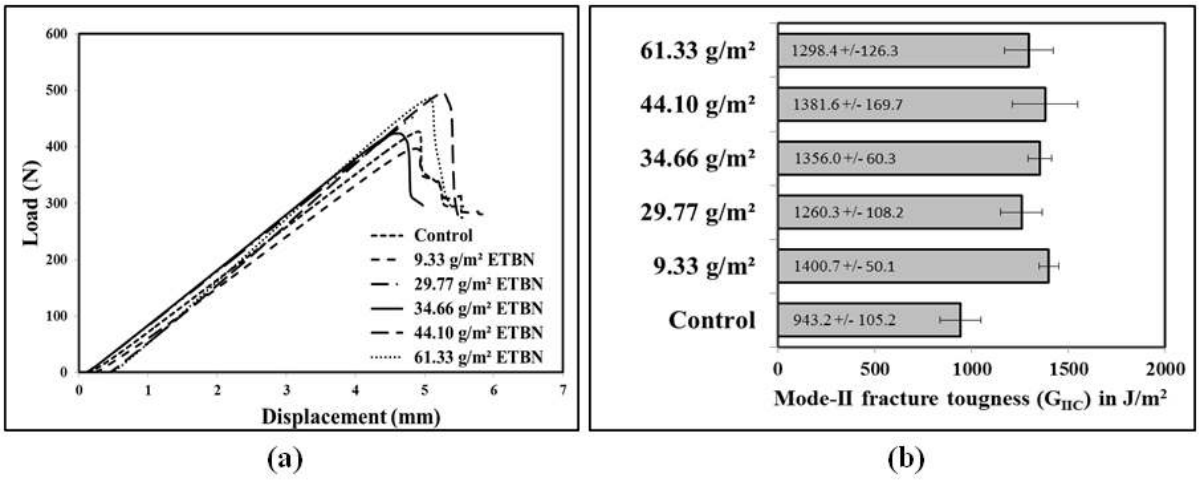

Fig 11.(a) Load vs. displacement curves - Mode-II fracture Test(b) Mode-II fracture toughness (G_{IIC})for control and rubber modified ENF specimens (error bars with standard deviation, minimum of 5 samples per data point).

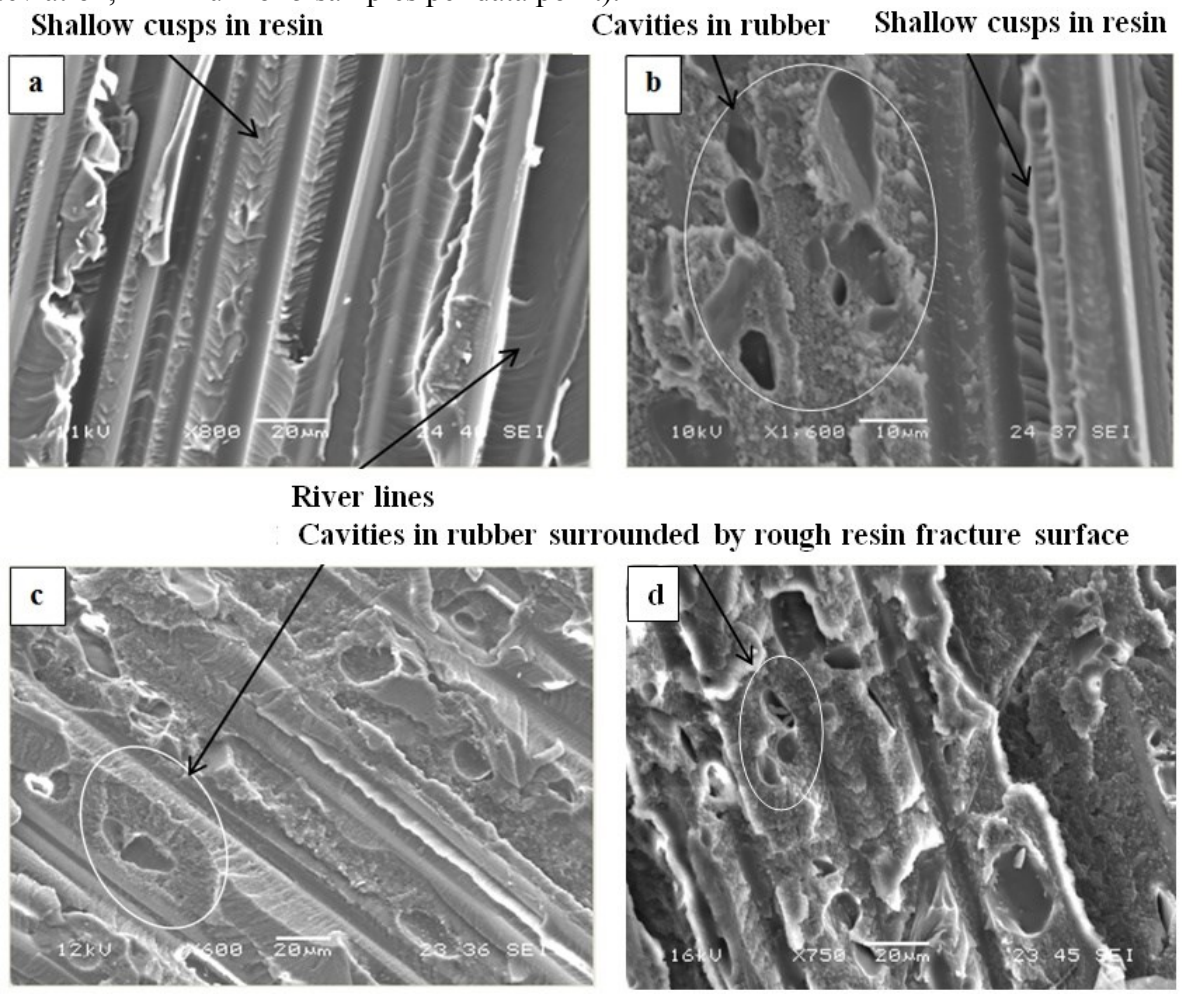

Fig 12. SEM micrographs for Mode-I fracture surface (a) control (b) 9.33 g/m^2 ETBN coated specimens (c) 29.77 g/m^2 ETBN coated specimens and (d) 34.66 g/m^2 ETBN coated specimens.

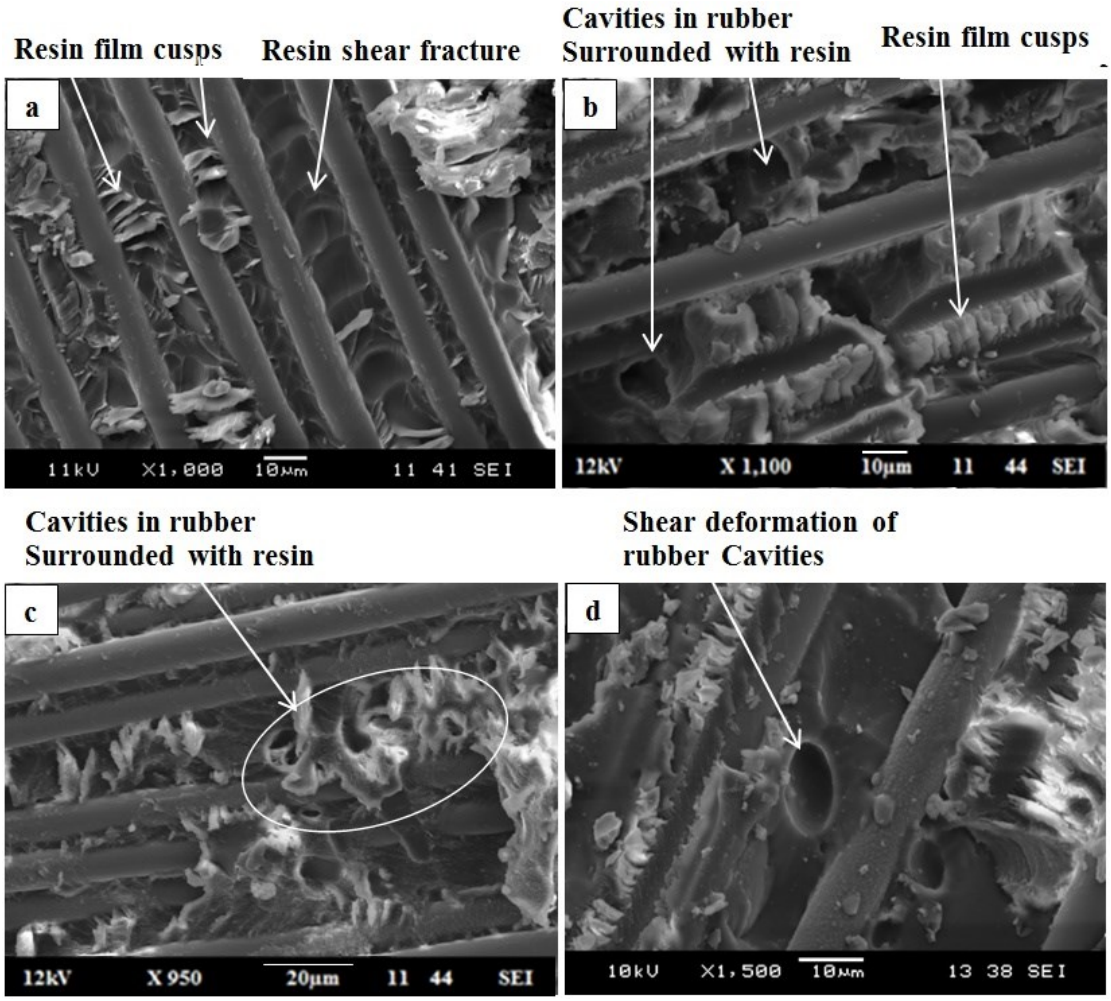

Fig 13. SEM micrographs of Mode-II fracture surfaces (a) control specimens (b) 34.66 g/m^2 ETBN coated specimens (c) 44 g/m^2 ETBN coated specimens and(d) 61.33 g/m^2 ETBN coated specimens.

Table.1 Rubber formulation with THF

Samples	ETBN Rubber content in wt%
Mode-I, DCB	14.25
	20.00
Mode-II, ENF	14.25
	20.00
	33.00
	40.00

Table 2 Measured coating density with respect to ETBN concentration

ETBN Rubber content in wt%	Wire winded on draw bar (Fig.1)	Measured aerial coating density (g/m^2)
14.25	0.2mm	9.33
	0.5mm	29.77
20.00	0.5mm	34.66
33.00	0.8mm	44.00
40.00	0.8mm	61.33

Table 3: Data obtained from DMA thermograms for epoxy-glass pre-preg laminates

Storage modulus (MPa)						
Sample	**50^0C**	**100^0C**	**150^0C**	**200^0C**	**250^0C**	**Tg (^{0}C)**
Glass control	15267	14359	7307	1181	1006	175
9.33 g/m^2 ETBN	14561	13470	7074	1094	942	175
29.77 g/m^2 ETBN	14351	13293	6888	1091	942	172
34.66 g/m^2 ETBN	13708	12856	6443	1089	934	175

Table.4: Literature values of G_{IC} and G_{IIC} Improvement with rubber modification

Rubber content (wt %)	Manufacturing Method	G_{IC} Improvement (%)	G_{IIC} Improvement (%)	Reference
CTBN (10)	Rubber Mixed with epoxy resin followed by RTM	22	Not reported	[16]
CTBN (15)	Rubber Mixed with epoxy resin followed by vacuum-assisted hand lay-up	112	Not reported	[17]
ETBN(14.25)	Draw down coating of rubber followed by Autoclave curing	122	49	From present study